Wind and Structures, *Vol. 19, No. 6 (2014) 585-601*
DOI: http://dx.doi.org/10.12989/was.2014.19.6.585

Numerical evaluation of the effect of multiple roughness changes

Daniel S. Abdi* and Girma T. Bitsuamlak

Department of Civil and Environmental Engineering, University of Western Ontario, 1151 Richmond St, London, ON N6A 3K7, Canada

(Received July 26, 2013, Revised March 7, 2014, Accepted March 31, 2014)

Abstract. The effect of multiple roughness changes close to a building site was examined through three dimensional computational fluid dynamics (CFD) simulations conducted in a virtual boundary layer wind tunnel (V-BLWT). The results obtained were compared with existing wind speed models, namely ESDU-82026 and Wang and Stathopoulos (WS) model. The latter was verified by wind tunnel tests of sixty nine cases of multiple roughness patches, and also with a simplified 2D numerical model. This work extends that numerical study to three dimensions and also models roughness elements explicitly. The current numerical study shows better agreement with the WS model, that has shown better agreements with BLWT tests, than the ESDU model. This is in contrast to previous results of Wang and Stathopoulos, who concluded that CFD shows better agreement with the ESDU model. Many cases were simulated in a V-BLWT that has same dimensions as BLWT used in the original experiment and also in a reduced symmetrical version (S-BLWT) that takes advantage of regular arrangement of roughness blocks. The S-BLWT gives results almost identical to V-BLWT simulations, while achieving significant reduction on computational time and resources.

Keywords: computational fluid dynamics; virtual BLWT; inhomogeneous roughness; ESDU wind speed model; Wang and Stathopoulos wind speed model; explicit roughness modeling

1. Introduction

Wind flow over terrain is affected by surface roughness characteristics as well as presence of topographic features. Proper evaluation of wind speed and turbulence intensity profiles is important for determination of wind loads on buildings, pedestrian level wind comfort studies, wind induced dispersion of pollutants etc. Both profiles are sensitive to upwind roughness changes especially close to a building site. Past studies assumed that the wind profile senses roughness in an averaged manner regardless of the distance of the roughness patch from the site (Grimmond and Oke 1999, Wieringa 1986). The significance of the effect of inhomogeneous roughness within the pertinent fetch is not addressed well in many building codes and standards. The earliest investigation of this effect was done by Deaves (1981), Deaves and Harris (1978) using simplified CFD simulations over single roughness changes. The result of their work is now incorporated in

*Corresponding author, Ph.D. Student, E-mail: dabdi3@uwo.ca
[a] Associate Professor, Email: gbitsuam@uwo.ca

http://www.techno-press.org/?journal=was&subpage=8 ISSN: 1226-6116 (Print), 1598-6225 (Online)

ESDU-82026 (1993), ESDU-84030 (1993) model for multiple roughness changes, which in turn has become one of the recommendations in many building codes and standards, along with experimental studies in boundary-layer wind tunnels.

Recently Wang and Stathopoulos (2007) put forward alternative wind speed and turbulence intensity models that improved upon the ESDU model. The model was validated with wind tunnel experiments and simplified two-dimensional CFD simulations over multiple roughness changes. The motivation for this new model was that the ESDU model can sometimes overestimate wind speed by as much as 20%, which translates to a 40% increase in wind load. Moreover the model's equations are much simpler than that of the ESDU model.

Other researchers have tried to tackle the problem using analytical means (Weng *et al*. 2010), 2D numerical simulations (Savelyev and Taylor 2005), and wind tunnel tests (Bradley 1968). The latter's findings regarding the variation of shear stress (Eq. (1)) are used in the numerical model of Wang and Stathopoulos for Smooth to Rough Case (S-R).

$$U_*(x) \propto x^{-0.1} \quad \text{for S-R} \tag{1}$$

The boundary layer in case of multiple roughness changes is stratified with an upper boundary layer that extends up to the gradient height, and as many inner boundary layers (IBLs) as there are roughness patches, with a possible transitional layer in between the IBLs. The case of a single roughness change with a transition layer is shown in Fig. 1. Three distinct regions can be observed, namely the outer layer, the transition layer and the internal boundary layer. The transition layer signifies the region affected by roughness conditions both upstream and downstream of the transition point.

CFD has been successful in wind engineering for pedestrian level wind comfort studies and to some extent for estimating mean wind loads. However its use for estimating peak wind loads is still under investigation using both wind-tunnel and full-scale experiments for validation. A review of the state of the art of CFD for wind-loading application can be found in Dagnew and Bitsuamlak (2013) among others. This work evaluates the performance of three dimensional CFD simulations, for the case of multiple roughness patches upstream of a building. Comparison is made with the above discussed models with regard to its ability to predict wind speed and turbulence intensity profiles reaching the face of the building.

Roughness elements are modeled explicitly and no assumption is made on the variation of shear stress from the transition point.

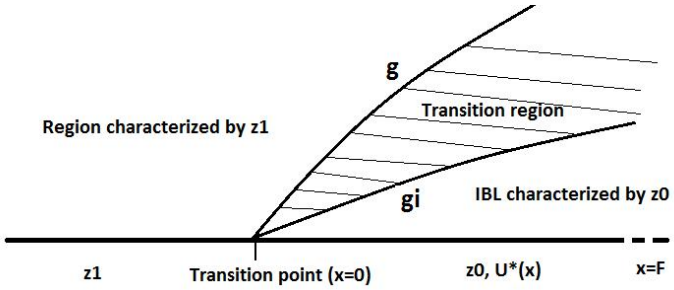

Fig. 1 Growth of IBL in single roughness change. Modified from Deaves (1981)

1.1 ESDU model

The set of equations provided in ESDU-82026 and ESDU-84030, for determining wind speed and turbulence intensity respectively for multiple roughness changes, are based on the numerical work of Deaves (1981). The ESDU model is now adopted in several building codes and standards such as ASCE-7 and NBCC. Deaves conducted CFD simulations using simple eddy viscosity (mixing length) models for turbulence closure. Contemporary CFD studies dropped the second horizontal derivatives rendering the Navier-Stokes equations parabolic and solutions were carried out by 'marching'. Deaves solved the full elliptic set of equations in which Coriolis force is also included using an approximation that allows the equations to remain two dimensional. These early efforts demonstrated the need for simplifications of CFD models mainly due to limitations in computational resources. It is the authors' opinion that computational technology has now advanced enough to allow for evaluation of roughness effects without simplifications such as use of zero-equation turbulence models, and empirical models for the variation of shear stress etc.

The ESDU-82026 wind speed model equations are briefly outlined below. The velocity profile within each IBL , $g_n <= z <= g_{n-1}$, can be calculated using the following equation

$$U(z) = K_{x2}K_{x3}K_{x4} \ldots K_{xn}U_n(z) \tag{2}$$

where K is a terrain dependent coefficient calculated differently for smooth to rough (S-R) and rough to smooth (R-S) transitions. The procedure for calculating K for multiple roughness patches numbered 1...n is outlined below. Given roughness characteristics of patch with ID *i*, namely, roughness length $z_{0,i}$ and patch length X_i

$$E = \log_{10} X; \qquad \text{where } X = X_2 + X_3 + \quad + X_i$$

$$f_{S-R} = \begin{cases} 0.1143E^2 + 1.372E + 4.087, if, E \le 5.5 \\ 0, if, E > 5.5 \end{cases}$$

$$f_{R-S} = \begin{cases} 0.0192E^2 - 0.550E + 2.477, if, E \le 5.6 \\ 0, if, E > 5.6 \end{cases}$$

$$R_i = \frac{[\ln(\frac{z_{0,i}-1}{z_{0,i}})]}{(\frac{u_*}{f z_{0,i}})_i^{\beta}} \quad \text{where } \beta = \begin{cases} 0.23, for, S-R \\ 0.14, for, R-S \end{cases}$$

$$K_{xi} = 1 + 0.67R_i^{0.85} f_{S-R}$$

$$K_{xi} = 1 - 0.41R_i f_{R-S} \tag{3}$$

Then the IBL depths $g_i(x)$ can be determined from continuity requirement at the location of roughness change. Two velocity profiles from different roughness characteristics are combined into one continuous profile using the following equation.

$$g_i(x) = \exp\left(\frac{K_{xi}(\frac{u_{*i}}{u_{*i-1}})\ln(z_{0,i}) - \ln(z_{0,i-1})}{K_{xi}(\frac{u_{*i}}{u_{*i-1}}) - 1}\right) \tag{4}$$

It is recommended that these equations should not be used for more than three patches, mainly due to lack of sufficient experimental validation.

1.2 Wang and Stathopoulos model

This model assumes segments of the IBL follow power law models. Unlike the ESDU model that is a single continuous curve, each segment of the wind profile has a wind speed curve dictated solely by the power law index of a corresponding patch. The wind speed model for each segment of the profile is then

$$U(z) = U(g_n(x))(\frac{z}{z_{g_n}})^{\alpha_n} \quad \text{where} \quad g_{n+1} \le z \le g_n \tag{5}$$

The IBL growth is assumed to follow a power law with a coefficient of 0.8.

$$g_0(x) = G$$

$$g_n(x) = 0.5 z_{0,(n,n-1)}^{0.2} x_n^{0.8} \text{ where } z_{0,(n,n-1)} = \max(z_{0,n}, z_{0,n-1}) \tag{6}$$

This set of equations are clearly simpler to use than the ESDU model, and more importantly give better results than ESDU according to wind tunnel tests conducted by the researchers.

2. Three dimensional CFD simulations

The major objective of this study is to assess performance of three dimensional CFD simulations for multiple changes in roughness conditions close to a building site. Most CFD software incorporates the effect of roughness on the developed wind profile using the concept of equivalent sand grain roughness, where it is assumed that the roughness is dense and homogeneous. This method has problems when the surface is very rough because of conflicting requirements in CFD modeling. The first requirement is that a fine mesh should be used close to walls to resolve high gradients of flow quantities. The second requirement is that the first cell's height should be greater than the sand grain roughness height K_s for more accurate results. Blocken *et al*. (2007) discussed these problems and gave many recommendations, among which explicit modeling of larger roughness elements was one of them. This has been done by Miles & Westbury (2003) and leads to a significant improvement of the computed results compared to that obtained with an approach flow over a rough flat wall. Roughness blocks used in the CFD simulations correspond to those used in an actual BLWT. A smooth wall assumption can be used when roughness elements are explicitly modeled. The disadvantage of this approach is that computational power is potentially wasted on less important part of the domain, when it could have been used elsewhere in the central region, in which the primary object of study is located.

2.1 Preliminary investigations

The first step in the investigation was to calibrate configurations of roughness elements for basic roughness classes: open country, sub-urban and urban. This could be achieved by conducting multiple simulations with different block configurations until the desired wind profiles are obtained at a target downstream location, which in case of wind tunnel is the center of turntable.

This iterative process can be time consuming if data is not already available from previous wind tunnel tests. Abdi *et al*. (2009) discusses an artificial neural network approach to determine configuration of roughness features for a desired mean wind speed and turbulence intensity profiles. If only roughness blocks are used as roughness features, empirical formulas can be used to determine aerodynamic roughness length from the density of obstacles. For cubic obstacles of height H and spacing S, the area density ratio can be approximated by the following formula.

$$\lambda = \frac{1}{(1+\frac{S}{H})^2} \tag{7}$$

For example, a spacing S=1.5H between blocks gives λ = 16% from which the roughness length can be estimated to be about $z_0 = 0.5\lambda H = 0.08H$ using Lettau's (1969) empirical formula that was derived from full-scale tests. Many other empirical formulas that relate roughness length with average frontal and planar area density ratios are discussed in Grimmond and Oke (1999), MacDonald *et al*. (1998). These estimates were good starting points for the iterative CFD simulations over different configurations. Then the configurations for the basic roughness classes were determined by repeated simulations until the desired logarithmic law or power law profile was achieved. After that multiple roughness patches composed of these basic roughness classes could be analyzed.

A typical simulation result over multiple rows of regularly arranged blocks, shown in Fig. 2(f), suggests a reduction of computational domain could be achieved by exploiting symmetry. Indeed that is the case when the blocks are arranged either perfectly aligned, or in a staggered form. Also the boundary conditions on the side walls should be symmetry (slip walls) as well. If a no-slip wall boundary condition is used there, rows close to the side walls exhibit different flow behavior than those in the middle. It is clear that simulating one raw of obstacle arrays was sufficient if a time averaged turbulence model, such as the k-epsilon model, was used. A section passing through the center of the cubes, and another one passing through the center of the open space between two rows gave the same result as simulations carried out over multiple rows of obstacles.

2.1.1 Boundary conditions

Boundary conditions are important in CFD simulations because they represent the effect of the surroundings on the computational domain. They serve as cut-off planes dividing the area of interest for simulation, from that we do not want to include in the simulation. The type of boundary condition also affects the placement of the cut-off planes relative to the central region where primary object of study is placed. The computational domain can be divided into three regions according to Blocken *et al*. (2007), namely the central region where the test building and its surroundings are modeled as best as possible, and the upstream and downstream regions where the effect of obstacles is approximated through roughness elements. The other issue concerns consistency of boundary conditions with the profiles used at the inlet and the turbulence model used (O'Sullivan *et al*. 2011).

At the inlet of the computational domain fully developed equilibrium velocity and turbulence intensity profiles are applied. The profiles used should be consistent with the upstream surface roughness characteristics (Wieringa 1993). The velocity specified at the inlet should be maintained within the computational domain, until it reaches the face of the primary object of study. A

peculiar problem in atmospheric boundary layer (ABL) simulations is that maintaining horizontal homogeneity is difficult to achieve with current batch of CFD software. Richards and Hoxey (1993) have investigated this problem thoroughly and suggested boundary conditions (Eqs. (8)-(10)) for the inlet that satisfy horizontal homogeneity. Their formulas have been used by the wind engineering community for many years. However it is not enough to specify only inlet conditions to get a stream-wise homogeneous flow. The wall functions used at the surface should be compatible with the roughness of the upstream fetch outside the domain, and a driving shear stress should be applied at the top of the domain as well (Hargreaves and Wright 2007).

$$u = \frac{u_*}{\kappa} \ln \frac{z + z_0}{z_0} \tag{8}$$

$$k = \frac{{u_*}^2}{\sqrt{C_\mu}} \tag{9}$$

$$\varepsilon = \frac{{u_*}^3}{\kappa(z + z_0)} \tag{10}$$

Richards and Hoxey found that the transport equations for the standard k-epsilon model could be satisfied with the above relations only when a different σ_e is used than the standard value of 1.3. The formula for calculating σ_e, given von Karman's constant is

$$\sigma_\varepsilon = \frac{\kappa^2}{(C_{\varepsilon 2} - C_{\varepsilon 1})\sqrt{C_\mu}} \tag{11}$$

Nikurdase's modified log-law Eqs. (12) and (13) are used as rough wall functions in many CFD code. As described in Blocken *et al*. (2007), the first cell's center should be placed higher than the equivalent sand grain roughness height i.e., $Y_p > K_s$. This constraint is in conflict with using a fine mesh close to walls where high velocity gradients are present.

$$u^+ = \frac{1}{\kappa} \ln(Ey^+) - \Delta B \tag{12}$$

$$\Delta B = \frac{1}{\kappa} \ln(1 + C_{ks} {K_s}^+) \tag{13}$$

For a horizontally homogeneous flow, i.e., one in which the velocity profile is maintained along the length of the domain, the wall function should approximately yield the same profile as the inlet profile as specified by Richards and Hoxey. Equating the above two equations for u^+ ,we get relations between K_s and z_0

$$u^+ = \frac{1}{\kappa} \ln \frac{z + z_0}{z_0} \quad \text{at inlet} \qquad \equiv \qquad u^+ = \frac{1}{\kappa} \ln\left(\frac{Ey^+}{1 + C_{ks} {K_s}^+}\right) \quad \text{at ground} \tag{14}$$

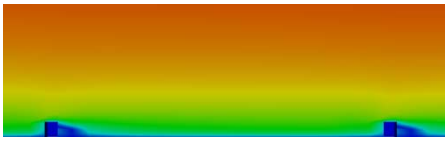

(a) open-no interference

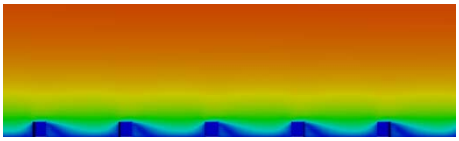

(b) suburban - wake interference

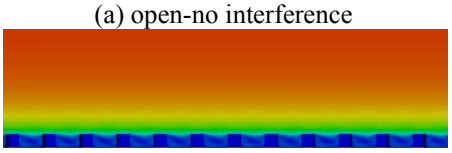

(c) urban-skimming flow

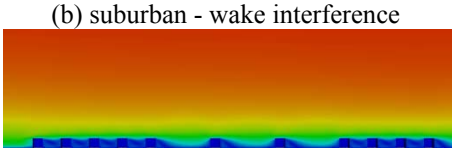

(d) multiple

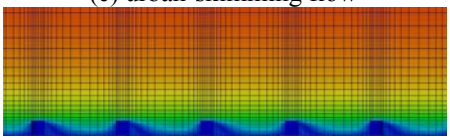

(e) mesh

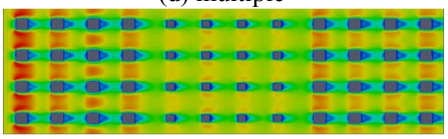

(f) plan of full domain

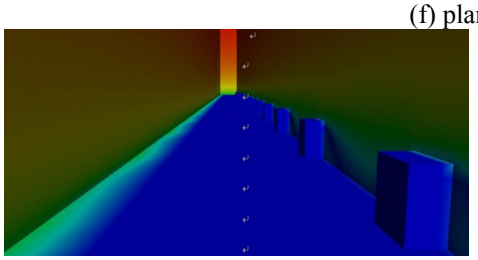

(g) Symmetrical computational domain

Fig. 2 Result of preliminary investigation: Velocity contours for different roughness patches

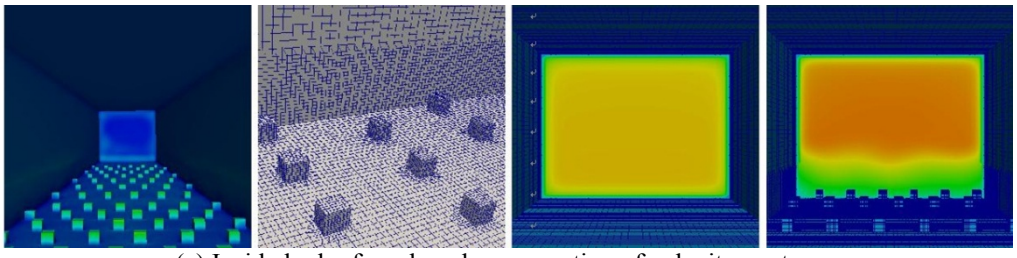

(a) Inside look of mesh and cross-section of velocity contours

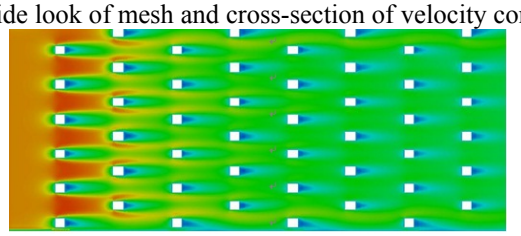

(b) Wakes development behind obstacles

Fig. 3 Virtual BLWT simulation result

$$\frac{z+z_0}{z_0}=\frac{Ey^+}{1+C_{ks}K_s{}^+}$$
$$\frac{z}{z_0}=\frac{Ey}{1+C_{ks}K_s}$$
$$K_s=\frac{Ez_0}{C_{ks}}$$
$$K_s\cong 20z_0 \tag{15}$$

At the sides and top of the domain, a symmetrical boundary condition that prevents inflow or outflow is usually applied. This boundary condition results in a parallel flow at the boundary, and could lead to artificial acceleration of flow, if enough space is not provided between the central region and the boundary plane. To solve this problem the domain must be sized in such a way that blockage ratio is below a certain limit, otherwise the result cannot be trusted due to significant blockage effect. Another solution is to replace the boundary condition with one that allows outward flow through the boundary plane (Franke and Hirsch 2004). Jimenez (2004) emphasizes the importance of the blockage ratio δ/h to the development of a logarithmic profile. For the current simulations δ=500 m and h=10 m, hence δ/h=50 or a blockage ratio of 2% is in the acceptable range. The ratio δ/h should be larger than 40 before similarity laws can be expected, and experimental results suggest that it should even be greater than 80.

The common use of symmetry boundary condition at the top of the boundary ignores the contribution of geostrophic wind in driving the ABL flow. Many researchers have noted that use of symmetry boundary condition results in stream-wise gradients of velocity profile. However there are reasons why symmetry is assumed in wind engineering problems. The major physical reason is that log layer in the ABL extends only up to a certain depth above which the gradient of velocity becomes zero. Also it is not known a priori what the values would be set at the top if symmetry boundary condition is not used. A driving shear stress boundary condition should be applied at the top to get a homogeneous (non-decaying) profile (Hargreaves and Wright 2007, O'Sullivan *et al*. 2011, Richards and Hoxey 1993). Another approach used by Bitsuamlak *et al*. (2006), Blocken *et al*. (2007) is to apply Dirichlet boundary condition for velocity and turbulence quantities at the top. The current study used this latter approach of fixing the flow quantities.

2.1.2 Reynolds number

The simulations are carried out in full scale dimensions. As discussed in the previous section, a wind speed profile consistent with the ground surface roughness is applied. For the case of open terrain roughness, a gradient wind speed of 16.75 m/s is reached at 240 m. The roughness blocks that are arranged in staggered manner have a height of 10m. The kinematic viscosity of air is 10^{-5} m^2/s, thus the Reynolds number of the flow is about $Re = 1.675 * 10^7$. The Reynolds number of the BLWT simulations discussed later are much lower than this value because model scale dimensions are used. Parameters such as Reynolds number and Jensen number are rarely perfectly matched in wind tunnel tests.

2.1.3 Results of preliminary investigation

We can observe three flow regimes, show in Fig. 2, which were first predicted by Oke (1998) for different packing of roughness elements. The first configuration corresponds to an open terrain

roughness condition where the spacing to height ratio of roughness elements is S/H~24. This case signifies an isolated flow regime where the wake and the separation bubble behind obstacles are fully developed with re-attachment occurring before the next element. With increased packing of obstacles, the roughness elements become close enough that wakes start to interfere with each other. The suburban roughness configuration with S/H~5 is in this wake interference regime. Increasing density of obstacles further to a very rough urban setting with S/H~1.7 leads to flow conditions known as 'skimming flow', where the flow is effectively displaced up by the height of obstacles. The present simulations used a constant height of blocks, varying only the spacing S to get different obstacle densities, thus the skimming flow effect is more pronounced than it would have been if variable height blocks were used. Zaki *et al*. (2010) has conducted wind tunnel measurements of roughness parameters of building arrays with random geometries (height and orientations), and concluded that skimming flow effect is absent.

2.2 Simulation of a BLWT with roughness features

Prior to a detailed study of multiple roughness patches using virtual BLWT, simulations are carried out with roughness features commonly used in BLWT, namely, roughness blocks, spires and barriers. This helps to understand the effect of each roughness feature better; later a decision is made to replace all of the roughness features at the entrance with an equilibrium boundary layer profiles. The flow in a wind tunnel is bounded by walls all around, similar to a case of pipe flow. It is important to check blockage ratio so that artificial accelerations of flow is minimal. Unlike the previous ABL simulation where symmetry boundary conditions are used at the sides and top of the domain, here it is more appropriate to use a no-slip boundary condition. All walls develop boundary layers though it can be very thin for smooth walls.

For this particular study the BLWT in the University of Western Ontario is used which has a test section of length 26 m, a width of 2.4 m and a variable height ranging from 1.55 m at the inlet to 2.15 m at the exit. The roughness features used are spires, barrier and roughness blocks. The computational domain is meshed with 2.6 million cells (480 x 40 x 40) generated using an automatic grid generation tool known as snappyHexMesh from OpenFOAM CFD. The tool first accepts a grid consisting of hexahedral elements and then modifies the near wall cells to polyhedral elements to better match the surface of irregular obstacles. Finally a specified number of layers, which in the current study is seven layers, of hexahedral elements are applied close to walls and edges of obstacles to capture the boundary layer flow better. The near wall cell's height is determined so that it center lies outside of the equivalent sand grain roughness height. First the case where none of these roughness features are used is considered, and the change in velocity profile due to the expansion of the tunnel alone is evaluated. The simulations are conducted with lower and higher number of cells than that mentioned above, and the results confirmed the current grid size is enough for a grid independent result. Therefore it can be said that the virtual BLWT wind tunnel is ready to add other roughness features or test objects at the turn table for further study.

After the simulation on open terrain, roughness blocks of height 0.1m are placed in a staggered manner and the mesh is refined towards the lower portion of the V-BLWT to capture effect of roughness blocks better. With each addition of roughness feature or test object, the mesh is refined more and more. As can be observed from Figs. 3 and 4, the boundary layer thickness on the bottom surface increases due to addition of the blocks. This is associated with an increase in turbulent kinetic energy as well. A planar view at about the height of blocks shows that each block

develops a wake that interferes with others. The interference effect in staggered arrangement is not as pronounced as that in regular arrangement where sheltering effect is maximum. Also the first couple of rows have the longest wakes, because there the wind starts to adjust to the new roughness conditions .

Next three spires and a barrier are added to help in development of boundary layer as early as possible. Again the mesh is refined for the spires because they lie outside of refinement zones applied so far. The barrier lies within the lower portions of the V-BLWT hence no further mesh refinements are required for it. If a uniform flow enters the tunnel, it is expected that a boundary layer will develop about $6H_s$ downstream of the spires. Fig. 5 shows the mesh and result of the analysis after the addition of these new roughness features. The boundary layer depth and turbulent kinetic energy has significantly increased compared to the case where blocks are the only roughness features. In a real boundary layer wind tunnel, the dimension of spires and height of barrier are used to control development of boundary layer profile. Both have significant impact over the wind profile reaching the turntable. Especially the wake from spires can be very elongated, hence care should be taken to avoid wake effects of spires from reaching the turntable.

2.3 Simulation of the cases of Wang and Stathopoulos with a virtual BLWT

The preliminary investigations highlighted procedures to be followed for studying roughness effects using CFD simulations over an array of blocks. Configurations for basic roughness classes have been determined and also the effect of different roughness features commonly used in BLWT have been assessed. In this section we investigate the effect of multiple roughness patches using configurations similar to that used by Wang and Stathopoulos. It is to be noted that even though the configuration for basic roughness patches are predetermined for this case, the work done in the preliminary investigations to determine basic configurations is a necessary step if it is not known a priori. Simulations are carried out for all the sixty nine cases of which a few are listed in Table 1. Each roughness patch is described by a letter describing the type of roughness, ’c’ for open, ’s’ for suburban and ’u’ for urban, followed by length of patch in meters at full scale (about 400x wind tunnel scale). Then virtual BLWT simulations are carried out without the use of spires and barrier. The reason for this choice is that we can directly apply the necessary inlet boundary layer profiles when conducting CFD simulations. However use of roughness features is mandatory in real wind tunnels because the flow is uniform at the inlet. The virtual BLWT used for this case is the one used by Wang and Stathopoulos, namely Concordia University BLWT which has a 12.2 m x 1.8 m x 1.8m working section. Roughness blocks were used to model suburban and urban roughness, while carpet was used to represent open country roughness. Some of the virtual BLWT setups and resulting velocity contours at the height of blocks are shown in Fig. 6.

Open country roughness is incorporated to the model by the use of wall functions, however the same method cannot be used for rougher patches as discussed in previous sections. Instead the approach of explicit modeling of roughness blocks is used for the suburban and urban roughness conditions. The roughness blocks used in Wang’s wind tunnel study were 1in cubes for suburban (S), and 1.5in cubes for urban (U). This configuration resulted in too many blocks, about18 across the width of the wind tunnel, therefore it was decided to double the size of the blocks to 2 in and 3 in respectively to reduce the number of roughness blocks. Empirical formulas that relate roughness length with size and spacing of blocks can be used to estimate the number of blocks required for a given roughness length. The modified configuration resulted in the same planar and frontal area density ratios as the original setup; hence they could be considered equivalent. To check this

proposition, a simulation is carried out for both configurations and the velocity profiles are compared. The results are almost identical - hence it was decided to use the modified configuration for the other cases as well. Other specifications, such as the wind speed, gradient height and friction velocity were duplicated in exactly the way the wind tunnel tests were carried out.

2.3.1 Results and discussion

The first simulations carried out on multiple roughness patches used a sand grain roughness K_s of 0.48 for open country roughness. The simulation result with that value of K_s soon revealed problems regarding scaling of roughness length. The problem concerns the location of the first cell closest to the ground. The center of the first cell $Y_p > 0.48$ is too high compared to the boundary layer thickness δ=0.6 m. This problem of matching roughness (Jensen number) and also dynamic forces (Reynolds number) in a BLWT is well known. Deviations from their full- scale values are usually acceptable to a certain extent for most wind engineering purposes. To avoid this problem with roughness matching, it was decided to use a much lower sand grain roughness for the carpet so that the condition $Y_p > K_s$ is satisfied. The simulations with $K_s = 0.48$ for open carpet typically showed a bulge in the velocity profile towards the ground, however using lower values corrected this problem and better results are obtained except in few cases where open country roughness dominates other roughness patches. In addition to the sand grain roughness that is now incompatible with the inlet profiles, a second problem exists, preventing formation of a horizontally homogeneous flow on carpet roughness. The boundary condition at the walls is a no-slip condition, instead of symmetry; thus the fluid will lose energy, and the wind speed profile will show some decay.

Then sixty-nine configurations, exactly as specified in Wang and Stathopoulos's study, were simulated in the virtual BLWT. The results for selected cases are shown in Fig. 6. One can observe that in most of the cases the virtual BLWT fits the WS model better than it does the ESDU model. This is in contrast to the result found by Wang and Stathopoulos using a two -dimensional numerical model that showed better agreements with the ESDU model.

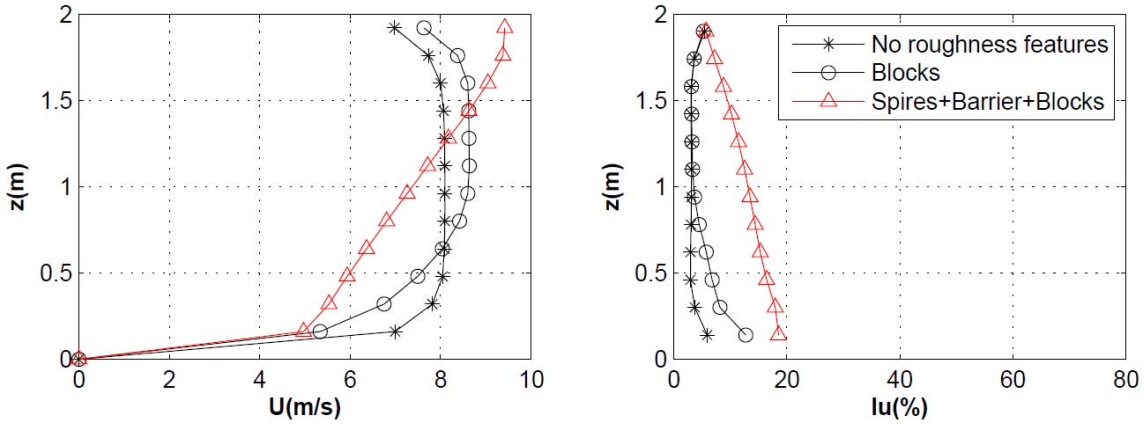

Fig. 4 Comparison of U and I_u profiles for different roughness features

Table 1 Few cases of multiple roughness patches

Case ID	Roughness patches (type(c/s/u) and length(m))
1	s 2000 c 125 s 250
2	s 2000 u 500 s 500
3	s 2000 u 125 s 125 u 125 s 125
4	s 2000 u 250 s 125
5	s 2000 c 125 s 125 c 125 s 125
6	s 2000 c 2250
7	c 2000 u 375 c 250
8	u 2000 c 2000

The numerical model of Wang and Stathopoulos used similar methodology to that of Deaves and Harris (1978), from which the ESDU model is developed, thus it is not surprising that the results showed better agreement with each other. The reason for the better performance of the current CFD model is not entirely due to the use of three-dimensional models, but mainly due to shear stress modeling used at the wall. Wang and Stathopoulos assumed a model of shear stress variation with fetch length as suggested by Bradley (1968). In addition the results of Garratt (1989), that the shear stress initially increase to about twice its equilibrium value for S-R change and decreases to about half its final value for R-S change, was also incorporated as follows

$$U_*(x) \propto 2x^{-0.1}U_* \quad \text{(for S-R)}$$

$$U_*(x) \propto 0.4x^{-0.1}U_* \quad \text{(for R-S)} \tag{16}$$

The current approach does not model the shear stress, but lets it be determined from the simulation. Also it should be noted that it is difficult to incorporate the WS numerical approach into an existing CFD software, due to the difficulty to apply shear stress model that varies with fetch length. The other difference concerns the turbulence models used. The WS numerical model used a linear eddy viscosity (mixing length) model for turbulence closure, while the current approach used two equation RANS turbulence models, namely, standard k-epsilon and RNG k-epsilon model. We believe that these two differences, though primarily the model of shear stress variation, are the reasons for better result found from virtual wind tunnel simulations.

2.4 Simulation of WS cases using simplified three dimensional models

The results of the virtual BLWT simulations suggest that computational effort can be reduced by taking advantage of symmetry of arrangement of the roughness elements. This is especially true for the rows in the middle that are farthest from the side walls. If the wind tunnel was infinitely wide, i.e., in the transverse direction, full symmetry of results can be achieved at all rows. Hence we can exploit symmetry by considering only two rows with the sides of the domain cutting

through the centerline of the rows. If the arrangement was regular, one row of blocks would have sufficed as outlined in the preliminary investigations and shown in Fig. 2. The symmetric BLWT (S-BLWT) represents an infinitely wide BLWT where as the V-BLWT represents an actual BLWT with limited width in which the side walls retard the flow for a no-slip boundary condition. If the side walls of V-BLWT are also slip walls, then the result of V-BLWT and S-BLWT should be exactly the same.

All the 69 cases of Wang and Stathopoulos were simulated again with this new setup. The simulation time decreases tremendously since the width of the tunnel is decreased by almost 35 times. The results are shown along with the virtual BLWT simulation results. We can observe that both wind speed and turbulence intensity results for the S-BLWT and V-BLWT are very close to one another. In very few cases the V-BLWT wind speed result matches the WS wind tunnel results slightly better than the S-BLWT, hence V-BLWT is the better model for reproducing actual wind tunnel results. However, the S-BLWT may actually be better in the grand scheme of things, because wind speed models over multiple roughness patches assume infinitely wide patches. Both the Wang and Stathopoulos, and ESDU models only take into consideration the length of a patch and its width.

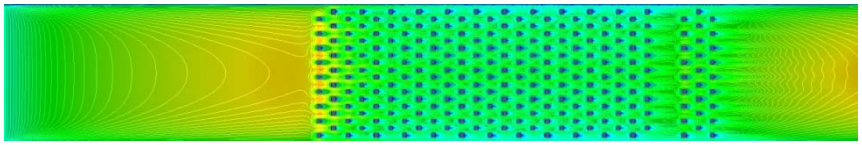

(a) Plan of V-BLWT case 1

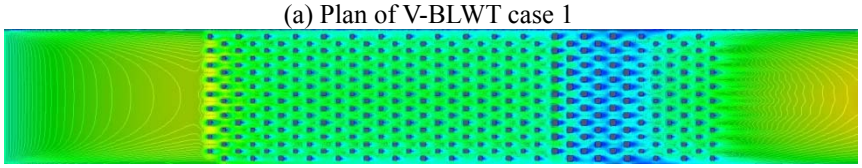

(b) Plan of V-BLWT case 2

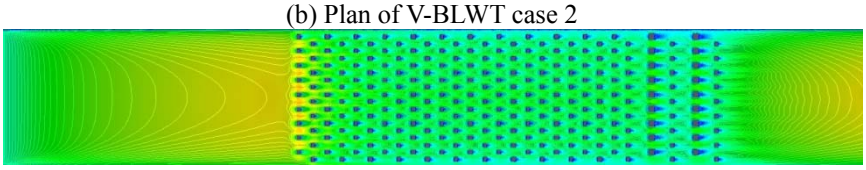

(c) Plan of V-BLWT case 3

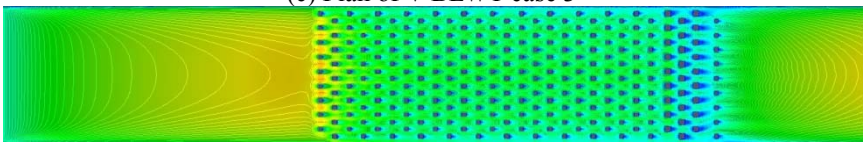

(d) Plan of V-BLWT case 4

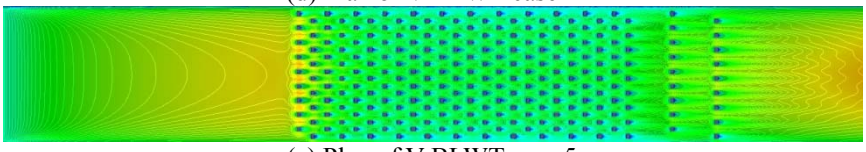

(e) Plan of V-BLWT case 5

Continued-

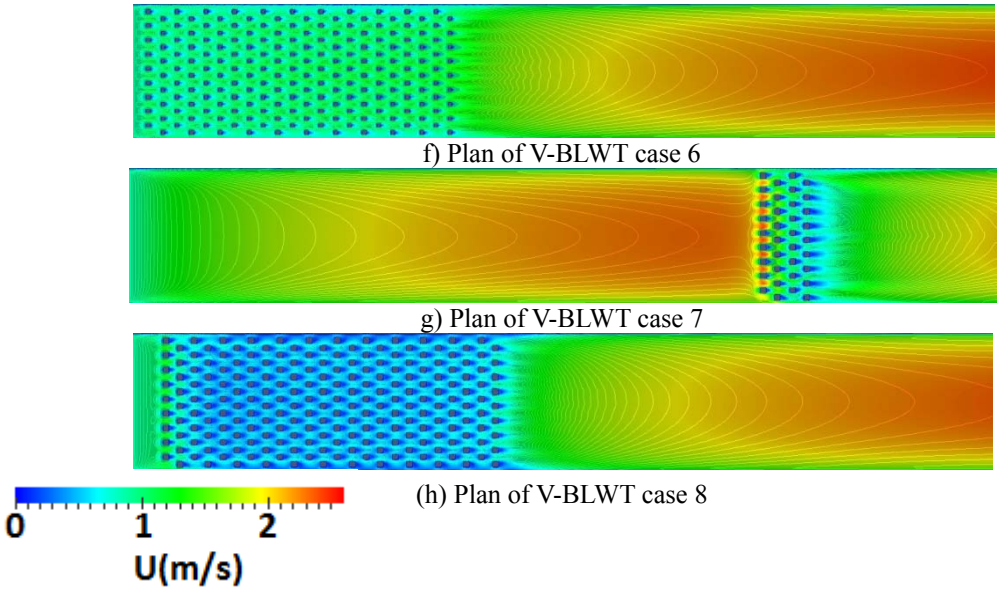

f) Plan of V-BLWT case 6

g) Plan of V-BLWT case 7

(h) Plan of V-BLWT case 8

Fig. 6 Virtual BLWT velocity contours at half height of blocks for selected cases shown in Table 1

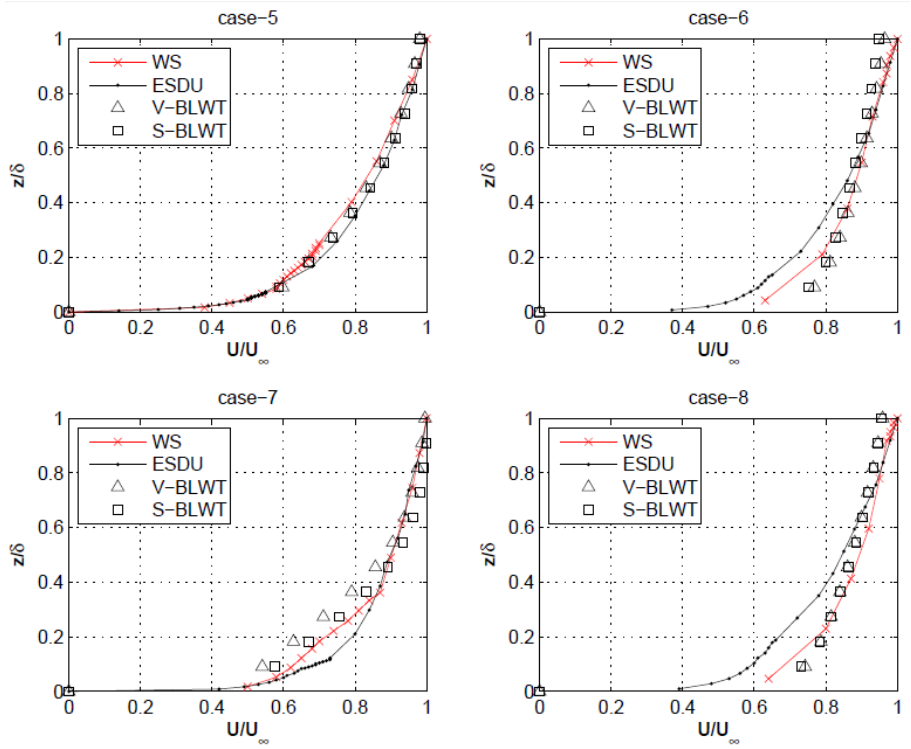

Fig. 7 Comparison of wind speed models with V-BLWT and S-BLWT

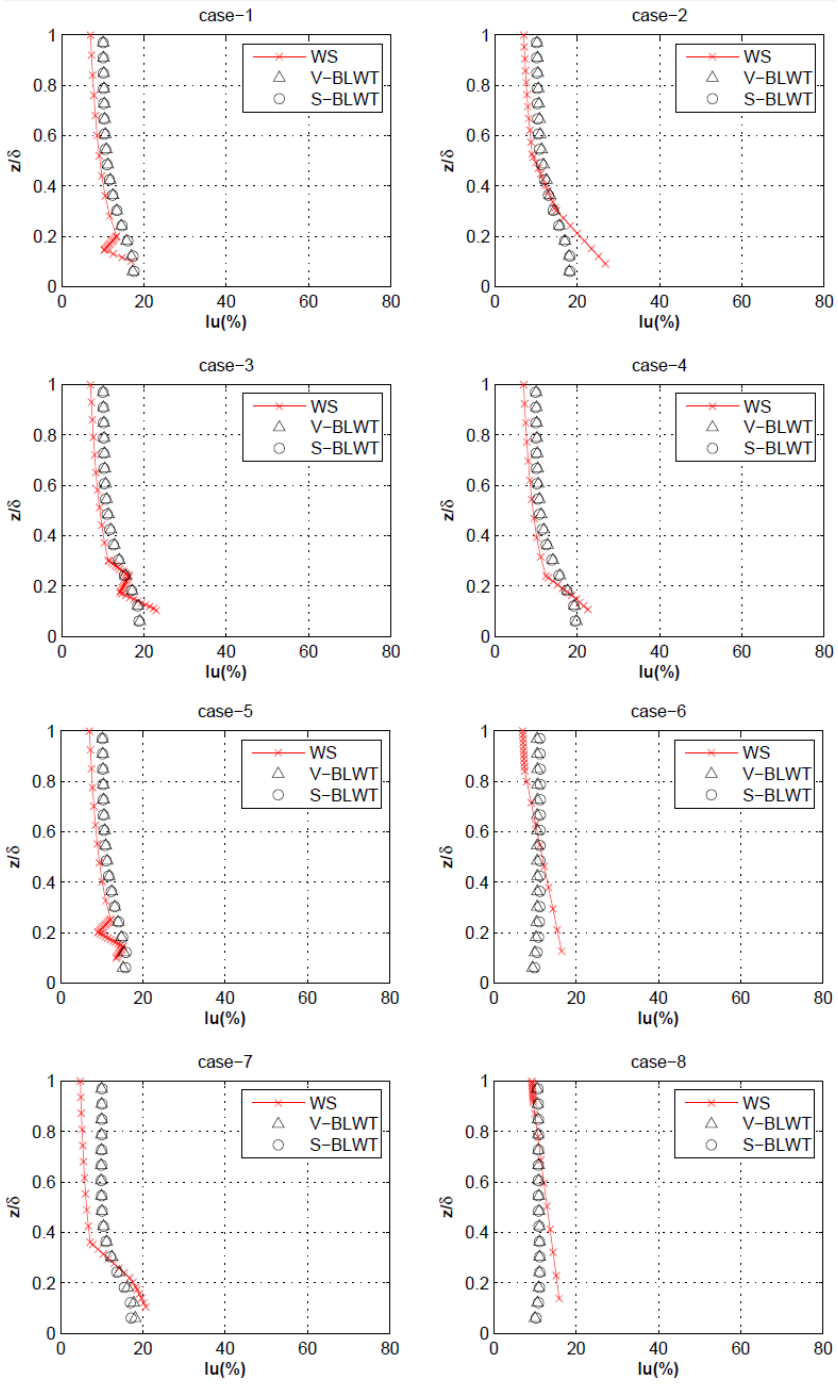

Fig. 8 Comparison of WS turbulence intensity model with V-BLWT and S-BLWT

3. Conclusions

Virtual boundary layer wind tunnel simulations have been used to evaluate the effects of multiple roughness changes close to a building site. The results obtained from simulation of multiple cases show better agreement with WS model than the ESDU model. Previous CFD studies concluded that better agreement is found with the ESDU model, but the current CFD study, that models roughness elements explicitly, contrasts with those earlier findings. This is mainly due to the use of a shear-stress model in previous numerical studies, which is avoided in this study by explicit modeling of roughness elements.

For the particular case of flow over staggered array of blocks, the virtual BLWT can be reduced further to effectively a single row of roughness elements (S-BLWT). The results obtained for this case are almost identical to the V-BLWT results for both wind speed and turbulence intensity profiles. Thus a significant reduction in computational resources can be achieved, without degrading the accuracy of the simulations. The S-BLWT cannot be used when a test object is placed on the turntable that breaks symmetry, or if more complex turbulence models, such as LES, are used.

On the other hand, the full virtual BLWT simulation can be used for other studies conducted in a boundary-layer wind tunnel. This work has demonstrated its use for evaluating multiple roughness changes close to a building. The results are encouraging and suggest other applications in which wind tunnel tests are routinely used. The effect of other roughness features has been briefly investigated, and for this particular study, using only roughness elements and applying fully developed boundary layer profile was found to be sufficient. This may not be appropriate for future studies using a virtual BLWT.

Acknowledgments

The authors would like to thank K. Wang and T. Stathopoulos for carrying out wind tunnel investigations of multiple roughness changes, without which the current numerical work would not have been possible. The many hours of simulations necessary for this work was provided by SHARCNET system at the University of Western Ontario. Last but not least the Canada Research Chair support for the second author is greatly acknowledged. Any opinions, findings, and conclusions or recommendations expressed in this material are those of the authors and do not necessarily reflect the views of the granting agencies.

References

Abdi, D., Levin, S. and Bitsuamlak, G. (2009), "Application of an artificial neural network model for boundary layer wind tunnel profile development", *Proceedings of the11th Americas Conference on Wind Engineering*

Bitsuamlak, G., Stathopoulos, T. and Bedard, C. (2006), "Effects of upstream two dimensional hills on design wind loads: a computational approach", *Wind Struct.*, **9**(1), 37-58.

Blocken, B., Stathopoulos, T. and Carmeliet, J. (2007), "CFD simulation of the atmospheric boundary layer: wall function problems", *J. Wind Eng. Ind. Aerod.*, **41**(2), 238-252.

Bradley, E.F. (1968), "A micrometeorological study of velocity profiles and surface drag in the region modified by a change in surface roughness", *Q. J. Roy. Meteorol. Soc.*, **94**(401), 361-379.

Dagnew, A.K. and Bitsuamlak, G.T. (2013), "Computational evaluation of wind loads on buildings: a review", *Wind Struct*., **16**(6), 629-660.
Deaves, D.M. (1981), "Computation of wind flow over changes in surface roughness", *J. Wind Eng. Ind. Aerod*., **7**(1), 65-94.
Deaves, D.M. and Harris, R.I. (1978), *A mathematical model of the structure of strong winds*, CIRIA report 76.
ESDU-82026 (1993), *Strong winds in the atmospheric boundary layer, Part 1: hourly-mean wind speeds*, ESDU International, London, U.K.
ESDU-84030 (1993), *Longitudinal turbulence intensities over terrain with multiple roughness changes*, ESDU International, London, U.K.
Franke, J. and Hirsch, C. (2004), "Recommendations on the use of CFD in wind engineering", *Proceedings of the International Conference in Urban Wind Engineering and Building Aerodynamics* .
Garratt, J.R. (1989), "The internal boundary layer - a review", *Bound. - Lay. Meteorol*., **50**(1-4), 171-203.
Grimmond, C.S.B. and Oke, T.R. (1999), "Aerodynamic properties of urban areas derived from analysis of surface form", *J. Appl. Meteor*., **38**, 1262-1292.
Hargreaves, D.M. and Wright, N.G. (2007), "On the use of k-epsilon model in commercial CFD software to model the atmospheric boundary layer", *J. Wind Eng. Ind. Aerod*., **95**, 355-369.
Jimenez, J. (2004), "Turbulent flow over rough walls", *Annu. Rev. Fluid Mech*., **36**, 173-196.
Lettau, H. (1969), "Note on aerodynamic roughness parameter estimation on the basis of roughness element description", *J. Appl. Meteor*., **8**, 828-833.
MacDonald, R.W., Griffiths, R.F. and Hall, D.J. (1998), "An improved method for the estimation of surface roughness of obstacle arrays", *Atmos. Environ*., **32**(11), 1857-1864.
Miles, S.D. and Westbury, P.S. (2003), *Practical tools for wind engineering in the built environment*, *The QNET-CFD Network Newsletter 2*.
Oke, T. (1998), "Street design and urban canopy layer climate", *Energy Build*., **103**(1-3), 103-113.
O'Sullivan, J., Archer, R. and Flay, R.G.J. (2011), "Consistent boundary conditions for flows within the atmospheric boundary layer", *J. Wind Eng. Ind. Aerod*., **99**(9), 66-67.
Richards, P.J. and Hoxey, R.P. (1993), "Appropriate boundary conditions for computational wind engineering models using the k-epsilon turbulence model", *J. Wind Eng. Ind. Aerod*., **46**,145-153.
Savelyev, S. and Taylor, P.A. (2005), "Internal boundary layers: 1. Height formulae for neutral and adiabatic flows", *Bound. - Lay. Meteorol*., **43**, 273-286.
Wang, K. and Stathopoulos, T. (2007), "Exposure model for wind loading of buildings", *J. Wind Eng. Ind. Aerod*., **95**(9-11), 1511-1525.
Weng, W., Taylor, P.A. and Salmon, J.R. (2010), "A 2-D numerical model of boundary-layer flow over single and multiple surface condition changes", *J. Wind Eng. Ind. Aerod*., **98**(3), 121-132.
Wieringa, J. (1986), "Roughness-dependent geographical interpolation of surface wind speed averages", *Q. J. Roy. Met. Soc.* **112**(473), 867-889.
Wieringa, J. (1993), "Representative roughness parameters for homogeneous terrain", *Bound. - Lay. Meteorol*., **63**, 323-363.
Zaki, S., Hagishma, A., Tanimoto, J. and Ikegaya, N. (2010), "Wind tunnel measurement of aerodynamic parameters of urban building arrays with random geometries", *Proceedings of the 5th International Symposium on Computational Wind Engineering*(*CWE2010).*

JH